

“No-Pair Bonding” in High-Spin Lithium Clusters: $n^+1\text{Li}_n$ ($n = 2-6$)

Sam P. de Visser, Yuval Alpert, David Danovich, and Sason Shaik*

Department of Organic Chemistry and the Lise Meitner-Minerva Center for Computational Quantum Chemistry, The Hebrew University of Jerusalem, 91904 Jerusalem, Israel

Received: July 31, 2000; In Final Form: September 14, 2000

High-spin lithium clusters ($n^+1\text{Li}_n$, $n = 2-6$) have been studied using several density functional methods. Although these high-spin clusters *have no bonding electron pairs*, they are stable with respect to isolated lithium atoms. Full geometry optimizations have been performed with alternatives under a variety of symmetry constraints which led to local minima. In general, the most stable structure is the one with the maximum coordination number for the lithium atoms. The agreement between B3P86/cc-pVDZ and B3PW91/cc-pVDZ density functional methods with UQCISD(T)/6-31G* and UCCSD(T)/cc-pVDZ calculations is excellent. Trends of bond dissociation energies are discussed as a function of total number of “bonds” and number of atoms.

1. Introduction

In the high-spin state, lithium can form clusters ($n^+1\text{Li}_n$) which are stable although there are no bonding electron-pairs.^{1,2} These type of clusters are higher in energy than the corresponding low-spin states but stable with respect to isolated lithium atoms. This is quite a surprising result as the triplet state of H_2 is not bound. The corresponding lithium cluster, on the contrary, is weakly bound with respect to two isolated lithium atoms. The binding energy of this lithium dimer (Li_2) is in the triplet state ($^3\Sigma_u^+$) 0.6 kcal mol⁻¹ at the UQCISD(T,fc)/6-31G*//UMP2-(full)/6-31G* level of theory¹ and 0.7 kcal mol⁻¹ at the UCCSD(T,full)/cc-pVDZ level of theory.²

Sizable clusters with high magnetic dipole moment are of interest to experimentalists. In addition, the form of bonding without electron pairs (“no pair bonding”) is puzzling and novel. Therefore, it was deemed essential to investigate larger no-pair bonded clusters $n^+1\text{Li}_n$ by means of density functional theory in order to establish a benchmark method for eventual studying larger clusters.

Lithium clusters in different spin states have been studied up to Li_6 by Glukhovtsev and Schleyer.¹ Their systematic study was primarily focused on ground state geometries of lithium clusters and involved mainly low spin states, but they also have studied some highly symmetrical $n^+1\text{Li}_n$ ($n = 2-6$) clusters. The latter clusters were restricted to structures in the highest symmetry, i.e., $^4\text{Li}_3$ (D_{3h} and $D_{\infty h}$ symmetry), $^5\text{Li}_4$ (T_d symmetry), $^6\text{Li}_5$ (C_{4v} and D_{3h} symmetry), and $^7\text{Li}_6$ (D_{4h} and D_{6h} symmetry). The most stable of these species was calculated on a level of theory up to UQCISD(T)/6-31G* with optimized geometries at the UMP2/6-31G* level of theory.

Because lithium is the smallest metallic atom with only three electrons, many calculations on lithium clusters are known from the literature. Most of these, though, deal with the lowest spin state of the system.³⁻¹¹

Boustani et al.³ did calculations on a large variety of lithium clusters in the lowest spin state. Geometries were optimized using Hartree–Fock theory with a minimal basis set (2s1p) with single point energy calculations at the multireference configuration interaction (MRD-CI) level of theory. They also studied

a few higher spin configurations but with their methods these systems were unstable with respect to isolated lithium atoms. Their calculations of the lithium dimer in the $^3\Sigma_u^+$ state predicted that this species is less stable than two isolated lithium atoms by 6.23 kcal mol⁻¹. Similarly, their calculations on $^4\text{Li}_3$ in the C_{2v} symmetry gave an unstable species by 4.04 kcal mol⁻¹ with respect to three isolated lithium atoms. The low spin geometries gave minimum energy values for the C_{2v} symmetrical structure for Li_3 , a parallelogram structure for Li_4 , a saw structure for Li_5 and a pyramidal structure for Li_6 . Low spin optimizations of Glukhovtsev and Schleyer¹ gave identical point groups for the minimum energy structures of Li_3 and Li_4 . The Li_5 cluster, however, was found to be a bipyramid in D_{3h} symmetry rather than the saw which Boustani et al found.

Blanc et al.⁴ did both experimental measurements and theoretical calculations on lithium clusters ($^1\text{Li}_n$, $n = 4, 6, 8$) and compared their absorption spectra with ones calculated using multireference single and double configuration interaction (MRSD-CI) and an atomic orbital basis sets of 13s3p/6s3p and 13s3p1d/6s3p1d. The most stable ground-state structures were assigned as a rhombic structure (D_{2h} symmetry) or a parallelogram for Li_4 and a C_{2v} symmetrical geometry for Li_6 .

A rigorous and systematic density functional study of small high-spin lithium clusters has never been performed. Therefore, we present here results of calculations on $n^+1\text{Li}_n$ clusters ($n = 2-6$). We will focus on the nature of the cluster, the bond dissociation energy per lithium atom and compare different density functional methods.

2. Theoretical Methods

All calculations presented here were performed with the Gaussian 98 program package.¹² Full geometry optimization followed by a complete frequency analyses was performed on high-spin lithium clusters, $n^+1\text{Li}_n$ ($n = 2-6$). Many different geometrical configurations were tested with a variety of symmetry groups. Whenever possible, calculations were run with a maximum symmetry constraint. The quality of different density functional methods was tested and compared with calculations from the literature. At least six hybrid density functionals were used on each geometry, i.e. B3LYP, B3P86, B3PW91, BLYP, BP86, and BPW91. Calculations were performed with either

* Corresponding author. Fax: +972-2-6585345. E-mail: sason@yfaat.ch.huji.ac.il.

TABLE 1: Bond Dissociation Energies (BDE) of ${}^3\text{Li}_2$ (${}^3\Sigma_u^+$) Calculated with Different DFT Methods and Basis Sets

method	cc-pVDZ BDE (kcal mol ⁻¹)	cc-pCVDZ BDE (kcal mol ⁻¹)	cc-pCVTZ BDE (kcal mol ⁻¹)
B3LYP	0.37	0.38	0.38
B3P86	1.68	1.67	1.68
B3PW91	1.26	1.26	1.26
BLYP	0.67	0.69	0.72
BP86	2.00	2.01	2.02
BPW91	1.88	1.88	1.87

Becke's exchange functional¹³ or Becke's three-parameter exchange functional.¹⁴ The functions for correlation were used from Perdew (P86),¹⁵ Lee, Yang, and Parr (LYP),¹⁶ or Perdew and Wang (PW91).¹⁷

The effect of the basis set was tested on the dimer using the cc-pVDZ, cc-pCVDZ and cc-pCVTZ basis sets.^{18,19} The first two basis sets also were used for the trimer. All calculations on higher clusters were restricted to the cc-pVDZ basis set, see text for details.

In all situations, atomic spin densities and Mulliken charges were checked in the output files and it was confirmed that no polarization effects occurred. Moreover, the atomic-atomic density was checked, thus confirming the lack of bonding electron pairs. Additionally, it was checked that the doubly occupied orbitals are 1s orbitals only.

3. Results

3.1. ${}^3\text{Li}_2$. The smallest lithium cluster is the dimer and in the high spin state (triplet) this species is only weakly bound. At the UQCISD(T,fc)/6-31G*//UMP2(full)/6-31G* level of theory, a bond dissociation energy of 0.55 kcal mol⁻¹ was found,¹ whereas calculations at the UCCSD(T,full)/cc-pVDZ level of theory gave 0.74 kcal mol⁻¹.² Details of the nature of the triplet no-pair bond can be found in ref 2; therefore, we will focus here only on the comparisons between the different methods and basis sets.

As a benchmark for the methods we have used here, we have calculated the lithium dimer in the triplet state using six different methods and three basis sets. The methods under study were the density functional methods: B3LYP, B3P86, B3PW91, BLYP, BP86, and BPW91. The basis sets were cc-pVDZ, cc-pCVDZ, and cc-pCVTZ. The details have been written in Table 1. As can be seen from these data is that the bond dissociation energy varies with less than 1% by changing the basis set within each method. This implies that a double- ζ basis function is sufficient to describe the high-spin lithium clusters. The different methods, though, give some scattered bond dissociation energies whereby the B3PW91 method overestimates the bond dissociation energy (BDE) and the B3LYP underestimates the BDE. The absolute values, though, are very small, and all methods fall within a range of 1 kcal mol⁻¹ from the literature values.^{1,2}

3.2. ${}^4\text{Li}_3$. The lithium trimer can be drawn in three possible configurations, i.e. a linear structure ($D_{\infty h}$ symmetry), an equilateral triangle (D_{3h} symmetry), and a nonequilateral triangle (C_{2v} symmetry). The first two structures have been studied with the six different methods and with two different basis sets (cc-pVDZ and cc-pCVDZ). The results of the calculations using the B3LYP, B3P86, B3PW91, BLYP, BP86, and BPW91 methods have been collected in Table 2. As can be seen from Table 2, the bond dissociation energies are essentially the same regardless of the choice of the basis set. Therefore, we have decided to continue the research on higher clusters with the smallest basis set only.

TABLE 2: DFT Bond Dissociation Energies (BDE) and Bond Distances of ${}^4\text{Li}_3$

	cc-pVDZ		cc-pCVDZ	
	BDE (kcal mol ⁻¹)	bond distance (Å)	BDE (kcal mol ⁻¹)	bond distance (Å)
linear (${}^4\Sigma_u$), $D_{\infty h}$				
B3LYP	2.6	3.412	2.5	3.428
B3P86	5.5	3.395	5.4	3.403
B3PW91	4.4	3.444	4.4	3.452
BLYP	3.7	3.360	3.5	3.378
BP86	6.3	3.391	6.3	3.399
BPW91	6.0	3.397	6.0	3.407
triangle (${}^4A_1'$), D_{3h}				
B3LYP	6.2	3.109	6.0	3.118
B3P86	11.0	3.092	10.8	3.091
B3PW91	9.4	3.131	9.3	3.131
BLYP	6.1	3.148	5.9	3.168
BP86	10.6	3.158	10.5	3.162
BPW91	10.2	3.165	10.1	3.170

The most stable quartet lithium trimer is the equilateral triangle. In addition to the linear and equilateral structures, a structure with C_{2v} symmetry has been considered since this structure is the lowest energy structure in the low-spin ground state which has doublet spin.^{1,3} Optimization of this nonequilateral triangle has only been performed with the B3LYP, B3P86, and B3PW91 methods and a cc-pVDZ basis set. All three optimizations, however, converge to a geometry with identical bond lengths and energies to the equilateral triangle and moreover have three angles of 60 degrees. A frequency analyses of the equilateral triangles gave positive frequencies only. Consequently, there is no stable quartet nonequilateral triangle as the optimizations relaxed toward an equilateral triangle with D_{3h} symmetry.

In contrast to the calculations of Glukhovtsev and Schleyer,¹ the linear configuration is a local minimum at the DFT levels. A frequency analysis gave positive frequencies only, whereas the calculations from ref 1 at the UHF/3-21G//UHF/3-21G level of theory gave a degenerate pair of imaginary frequencies. The reason for this inconsistency may be that our wave function converges to an electronic state with ${}^4\Sigma_u$ symmetry, whereas Glukhovtsev and Schleyer found an electronic state, of ${}^4\Sigma_g^+$ symmetry. In our case the doubly occupied orbitals represent two σ_g and one σ_u orbitals consisting the three 1s orbitals on each lithium atom. In an atomic orbital concept, the three singly occupied orbitals are the linear combinations $2s_1+2s_2+2s_3$, $2s_1-2s_3$, and $2s_1-2s_2+2s_3$ of the atomic orbitals and have symmetry σ_g , σ_u , and σ_g respectively. This leads to an electronic state of ${}^4\Sigma_u^+$. Consequently, the linear configuration in the calculations of Glukhovtsev and Schleyer will be an electronic excited state.

The lowest energy trimer is the equilateral triangle and is 4.9 kcal mol⁻¹ more stable than the linear configuration at the B3PW91/cc-pCVDZ level of theory.

Calculations of Glukhovtsev and Schleyer¹ on quartet lithium trimer in D_{3h} symmetry (${}^4A_1'$) at the UQCISD(T)(full)/6-311+G-(3df)//UMP2(full)/6-31+G* level of theory gave a bond dissociation energy of 11.5 kcal mol⁻¹ and at the UQCISD(T)(fc)/6-31+G*//UMP2(full)/6-31+G* 7.8 kcal mol⁻¹ was found. Our calculations using the B3P86 and B3PW91 levels of theory fall within the range of these two literature values. The B3LYP calculations give somewhat lower bond dissociation energies of 6.2 and 6.0 kcal mol⁻¹ using the cc-pVDZ and cc-pCVDZ basis sets, respectively. UCCSD(T)/cc-pVDZ calculations by Danovich et al.² gave a bond dissociation energy of 10.2 kcal mol⁻¹ which is midway between the B3P86 and B3PW91 results obtained from the present study. Consequently, the density

TABLE 3: DFT Bond Dissociation Energies (BDE) of Different ${}^5\text{Li}_4$ Geometries^a

	B3LYP BDE (kcal mol ⁻¹)	B3P86 BDE (kcal mol ⁻¹)	B3PW91 BDE (kcal mol ⁻¹)	BLYP BDE (kcal mol ⁻¹)	BP86 BDE (kcal mol ⁻¹)	BPW91 BDE (kcal mol ⁻¹)
linear ${}^5\Sigma_g, D_{\infty h}$ (0)	3.4	9.0	6.8	8.4	9.3	8.7
star ${}^5A_2'', D_{3h}$ (3) ^b	3.8	11.5	9.0	6.3	10.9	10.3
triangle with tail ${}^5B_2, C_{2v}$ (0)	8.9	15.2	13.0	9.3	15.2	14.7
parallelogram ${}^5A_u, D_{2h}$ (1)	10.6	19.5	16.9	10.3	18.9	18.4
square ${}^5B_{2g}, D_{4h}$ (0)	13.2	20.4	17.8	11.0	17.6	17.3
pyramid ${}^5A_1, T_d$ (0)	20.1	29.8	27.1	18.9	28.3	27.9

^a For structures see Figure 1. Near each structure the numbers in parentheses correspond to the number of imaginary frequencies. ^b Electronic state ${}^5A_1'$ (BLYP, BP86, BPW91); BLYP gave two imaginary frequencies.

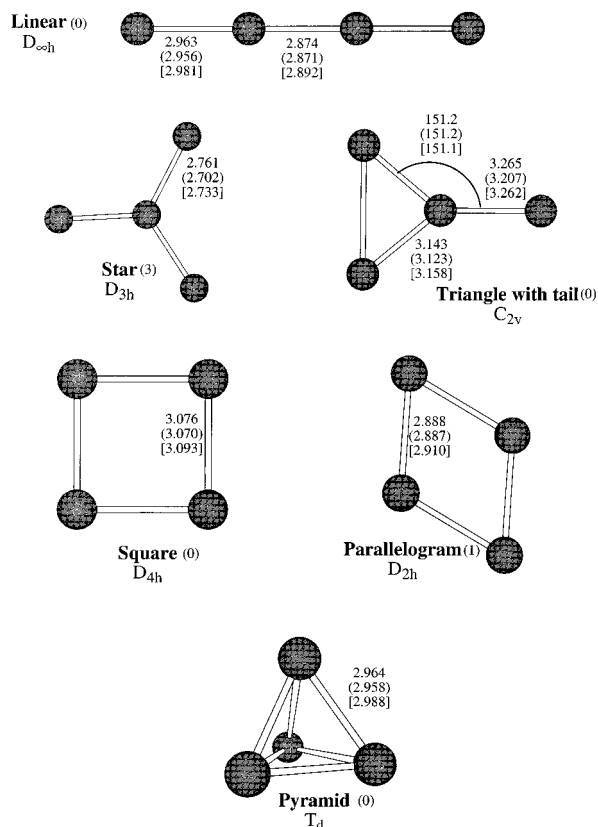


Figure 1. Optimized ${}^5\text{Li}_4$ structures with bond distances in angstroms calculated with B3LYP, B3P86 (brackets), and B3PW91 (square brackets).

functional methods B3P86 and B3PW91 reproduce bond dissociation energies of high level ab initio methods excellently.

The calculated bond distance of 3.167 Å from ref 1 is slightly longer than the values we obtained from our calculations, see Table 2. The B3PW91 calculations gave bond distances which were within 1% of the ones obtained by Glukhovtsev and Schleyer. The B3PW91 and B3P86 calculations gave an interatomic bond of 3.131 and 3.109 Å, respectively.

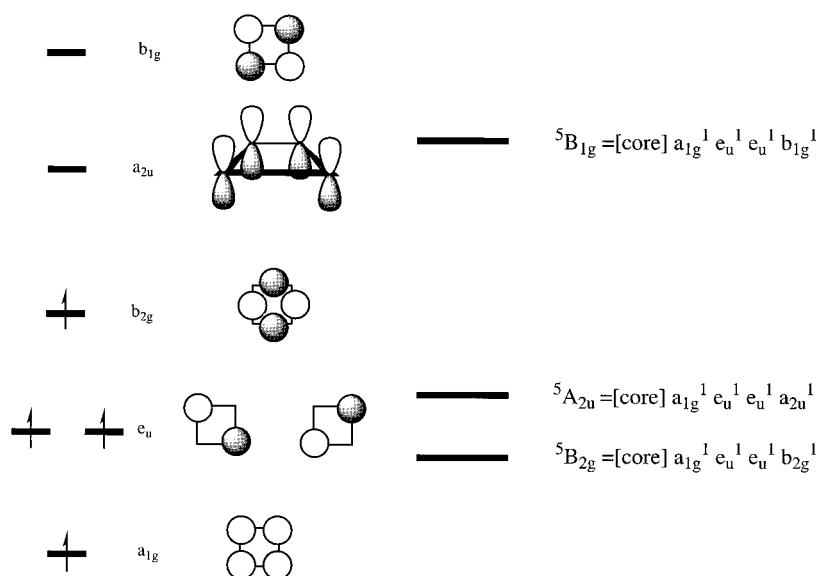
3.3. ${}^5\text{Li}_4$. Six different geometries have been tested for the quintet lithium tetramer, namely a linear configuration ($D_{\infty h}$ symmetry), a pyramid (T_d symmetry), a square (D_{4h} symmetry), a star (D_{3h} symmetry), a parallelogram (D_{2h} symmetry), and a triangle with a tail (C_{2v} symmetry). Optimized geometries are depicted in Figure 1. Bond dissociation energies (BDE) are given in Table 3 for the calculations involving the B3LYP, B3P86, B3PW91, BLYP, BP86, and BPW91 methods. All methods give the same bond dissociation energy trends, although the B3LYP and BLYP methods give significantly lower absolute BDEs.

The lowest energy structure is the pyramidal conformation and has a BDE = 27.1 kcal mol⁻¹ using the B3PW91 method,

whereas using the B3P86 method a BDE = 29.8 kcal mol⁻¹ with respect to four isolated lithium atoms has been obtained. This is in quite perfect agreement with the UCCSD(T) calculations from ref 2 of 29.6 kcal mol⁻¹. At the UQCISD(T)-(fc)/6-31G*/UMP2(full)/6-31G* level of theory Glukhovtsev and Schleyer¹ obtained a slightly lower BDE of 25.4 kcal mol⁻¹. Their optimized geometry had a lithium–lithium bond distance of 3.056 Å at the UMP2(full)/6-31G* level of theory, which is of the same order of magnitude as our results of 2.964 Å (B3LYP), 2.958 Å (B3P86), and 2.988 Å (B3PW91). The UCCSD(T) optimization gave an interatomic distance of 3.036 Å.

A second quintet geometry tested by Glukhovtsev and Schleyer was the square conformation. They optimized this geometry in the ${}^5A_{2u}$ state and found 4 imaginary frequencies indicating a higher order saddle point. Our initial calculations on the D_{4h} ${}^5A_{2u}$ state of the tetramer gave a second-order saddle point with a bond dissociation energy of 9.2 kcal mol⁻¹ (B3LYP), 17.8 kcal mol⁻¹ (B3P86), and 15.3 kcal mol⁻¹ (B3PW91). The ${}^5A_{2u}$ electronic state, however, is an excited quintet state in the square conformation. The singly occupied orbitals involved in this state have symmetry groups a_{1g} , e_u , e_u , and a_{2u} . The latter orbital is a linear combination of $2p_z$ orbitals. A lower lying electronic state is the ${}^5B_{2g}$ state which has four singly occupied σ orbitals. The highest singly occupied orbital with b_{2g} symmetry has the highest orbital density between the atoms! Not surprisingly, a huge amount of p-character is necessary to build the b_{2g} orbital. Calculations of McAdon and Goddard⁶ on larger lithium rings clusters in the high spin state at the UHF level of theory with a basis set (9s,4p)/(3s,2p) gave similar results. Their calculations on ${}^{11}\text{Li}_{10}$ ring gave an overall electronic state of ${}^{11}B_{2u}$ with the electronic densities in the highest singly occupied orbital between the atomic centers. Their attempts to optimize the ${}^{11}B_{1u}$ state (with the electronic densities located on the atomic centers) failed as the elementary excitation of $b_{1u} \leftarrow b_{2u}$ is totally repulsive.⁶ In the ${}^5\text{Li}_4$ (D_{4h}) system the analogous transition corresponds to a $b_{1g} \leftarrow b_{2g}$ excitation. The ${}^5B_{1g}$ electronic state is a linear combination of 2s orbitals and has the electron densities localized on the atomic centers. Our attempts to calculate the square conformation in the ${}^5B_{1g}$ electronic state have been performed using the B3LYP, B3P86 and B3PW91 methods, although the latter one did not converge. Using the B3LYP method the ${}^5B_{1g}$ electronic state is only slightly stable with respect to dissociation into lithium atoms as the bond dissociation energy has been found to be 0.9 kcal mol⁻¹. The B3P86 method converged to a BDE = 6.0 kcal mol⁻¹, which is 11.1 kcal mol⁻¹ higher in energy relative to the ${}^5A_{2u}$ electronic state and 13.6 kcal mol⁻¹ higher in energy relative to the ${}^5B_{2g}$ electronic state. Consequently, the order of the electronic states of the quintet squared lithium tetramer will be ${}^5B_{2g} < {}^5A_{2u} < {}^5B_{1g}$. On the left-hand-side of Scheme 1, the ordering of the molecular orbitals has been schematically

SCHEME 1

TABLE 4: DFT Bond Dissociation Energies (BDE) of Different ${}^6\text{Li}_5$ Geometries^a

	B3LYP BDE (kcal mol ⁻¹)	B3P86 BDE (kcal mol ⁻¹)	B3PW91 BDE (kcal mol ⁻¹)	BLYP BDE (kcal mol ⁻¹)	BP86 BDE (kcal mol ⁻¹)	BPW91 BDE (kcal mol ⁻¹)
linear ${}^6\Sigma_g, D_{\infty h}$ (0)	8.6	15.5	12.7	13.9	16.3	15.5
tetrahedral ${}^6A_1, T_d$ (5)	9.1	17.7	14.7	10.3	18.8	17.8
star ${}^6B_{1u}, D_{4h}$ (2) ^b	11.0	24.3	20.4	8.0	17.4	16.7
saw ${}^6A_2, C_{2v}$ (2) ^c	17.5	29.1	25.6	17.3	28.6	27.9
cyclo ${}^6A_1', D_{5h}$ (0)	23.3	32.0	28.6	20.5	28.4	27.8
bipyramid ${}^6A_2'', D_{3h}$ (2) ^d	23.0	35.7	31.9	22.6	35.0	34.1
pyramid ${}^6B_1, C_{4v}$ (1) ^e	23.8	36.7	33.0	21.5	33.9	33.5

^a For structures see Figure 2. Near each structure the numbers in parentheses correspond to the number of imaginary frequencies. ^b B3LYP gave four imaginary frequencies. ^c B3LYP gave one imaginary frequency. ^d BLYP gave no negative frequencies. ^e The true minimum is close to being pyramidal, explanation see text.

depicted with the shape of the orbitals next to the diagram. The occupation of the orbitals in the lowest quintet state (${}^5B_{2g}$) has been represented by arrows in the scheme, where the a_{1g} , e_u , e_u , and b_{2g} orbitals are singly occupied. A higher lying state (${}^5A_{2u}$) is obtained by the promotion of an electron from the b_{2g} orbital to the a_{2u} orbital, which is a linear combination of $2p_z$ orbitals. The ${}^5B_{1g}$ electronic state, on the contrary, lies even above this ${}^5A_{2u}$ state and is the result of an excitation of an electron from the b_{2g} to a b_{1g} orbital. The order of the electronic states of the quartet lithium tetramer is visualized on the right-hand-side of Scheme 1. In the quintet state the D_{4h} symmetrical structure is a stable minimum in the ${}^5B_{2g}$ electronic state with positive frequencies only, this in contrast to the two negative frequencies found for the ${}^5A_{2u}$ electronic state.

In the lowest spin state the parallelogram was found to be the lowest energy structure.^{3,4,10} At the quintet spin state this structure is a first-order saddle point with one imaginary frequency. Energetically, this configuration is 9.5, 10.4, and 10.2 kcal mol⁻¹ higher in energy as the pyramidal structure using the B3LYP, B3P86, and B3PW91 methods, respectively.

The linear configuration is a local minimum with positive frequencies only, but is considerably higher in energy as the most stable ${}^5\text{Li}_4$ structure by 16.6 kcal mol⁻¹, 20.8 kcal mol⁻¹ and 20.3 kcal mol⁻¹ using the B3LYP, B3P86, and B3PW91 methods, respectively. The C_{2v} symmetrical structure is also a local minimum although at the B3P86 level of theory a small but negative frequency ($i17\text{ cm}^{-1}$) is obtained. Using all other methods only positive frequencies are found. We conclude therefore, that this C_{2v} symmetrical structure is a local minimum.

The bond dissociation energy of this structure is roughly half the value of the most stable tetramer, i.e., the pyramid.

3.4. ${}^6\text{Li}_5$. Sextet lithium pentamer geometries have been optimized under seven high-symmetry constraints, i.e., $D_{\infty h}$ (linear structure), D_{5h} (cyclic structure), D_{4h} (star-shaped structure), D_{3h} (bipyramid), T_d (tetrahedral), C_{4v} (pyramid), and C_{2v} (saw). Optimized geometries at the B3LYP, B3P86, and B3PW91 levels of theory are schematically depicted in Figure 2, whereas bond dissociation energies (BDE) of the results of all tested methods are written in Table 4.

The bond dissociation energy (BDE) trends are essentially the same for the methods B3LYP, B3P86, and B3PW91 methods. In most cases, the BP86 and BPW91 methods follow the same trends as the Becke three-parameter calculations, although with one important exception, namely, the most stable form. In particular, the results from the BLYP calculations are quite displaced from the calculations using the other methods and therefore must be treated with great care. First, the BDE trend is distorted compared to the B3LYP trend. The stability of the local linear minimum is enhanced by 5.3 kcal mol⁻¹. In addition, the most stable minimum is the bipyramid. The BP86 and BPW91 also have the bipyramidal structure as the lowest energy structure, but these methods give one imaginary frequency. An optimization started with the optimized BP86 and BPW91 bipyramidal structure with the Cartesian coordinates of the normal mode of the imaginary frequency added leads to a minimum energy structure calculated using these methods with only positive frequencies and C_2 symmetry. Geometrically, this C_2 symmetrical structure is a strongly distorted pyramid with a

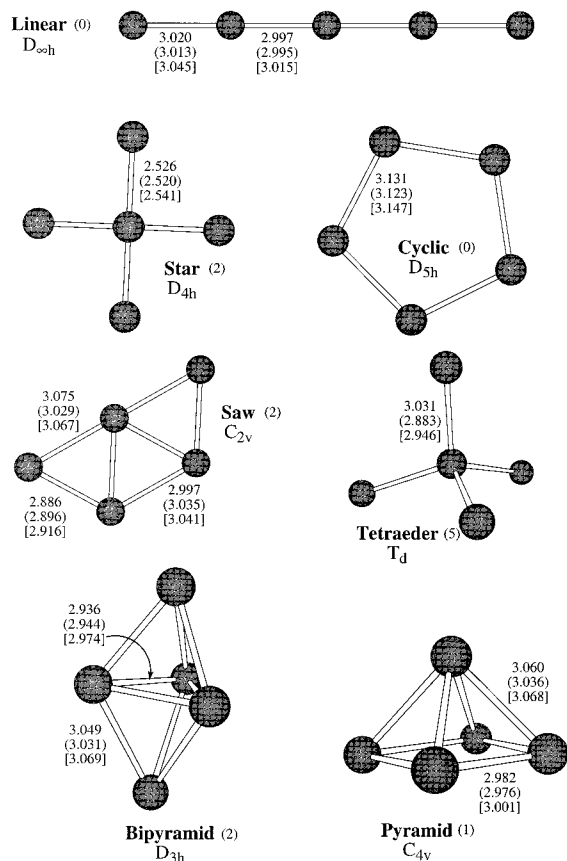


Figure 2. Optimized ${}^6\text{Li}_5$ structures with bond distances in angstroms calculated with B3LYP, B3P86 (brackets) and B3PW91 (square brackets).

nonplanar ground surface. Attempts to optimize this structure with B3LYP, B3P86 and B3PW91 lead to a structure which closely resembles the pyramidal structure. As the higher level calculations with the Becke three-parameter method give a different minimum energy structure than the BLYP, BP86, and BPW91 calculations, the latter ones must be considered as less suitable for the type of calculations presented here. Consequently, the C_2 optimized structure using the BLYP, BP86 and BPW91 methods must be seen as an artifact. Therefore, these three methods have not been used for the higher lithium clusters with six lithium atoms.

The lowest energy structure using the B3LYP, B3P86 and B3PW91 methods is the pyramid which still has one imaginary frequency. An intrinsic reaction coordinate (IRC) calculation starting from this point converges to a minimum after 5 steps. This implies that the true minimum is very close to this pyramidal configuration. In addition to the IRC calculation, we also have performed an optimization using the Cartesian coordinates of the optimized structure plus the Cartesian coordinates of the imaginary frequency. This reduced the symmetry from C_{4v} to C_{2v} . Calculations of the C_{2v} structure using the B3LYP, B3P86, and B3PW91 methods converged to a minimum energy structure with positive frequencies only. The obtained bond dissociation energies are 23.8, 36.7, and 33.0 kcal mol $^{-1}$, respectively. Furthermore, the atomic bond distances are close to the ones obtained for the C_{4v} symmetry. The bond distance r_{12} augments with 4% whereas r_{14} decreases with the same value. Consequently, the pyramidal structure is the lowest energy structure and is close to being C_{4v} symmetry.

Despite two negative frequencies, the bipyrmaidal structure in the sextet spin state is just 0.8, 1.0, and 1.1 kcal mol $^{-1}$ higher

in energy as the most stable sextet structure, i.e., the pyramid, using the B3LYP, B3P86, and B3PW91 methods, respectively. The two negative frequencies represent a degenerate pair of frequencies with e'' symmetry. At the B3PW91 level of theory these frequencies are -195 cm $^{-1}$, and at the B3P86 level of theory they are -201 cm $^{-1}$. A geometry optimization of a structure composed of the Cartesian coordinates of the optimized bipyrmaid and the coordinates of the lowest frequency gave a structure with C_2 symmetry which converged to a geometry which closely resembles the pyramid. Energetically, these C_2 and C_{4v} structures are identical. In conclusion, the bipyrmaid with D_{3h} symmetry is a transition state leading toward the pyramidal structure.

The UCCSD(T)/cc-pVDZ calculations² on the pyramidal structure gave a bond dissociation energy of 35.4 kcal mol $^{-1}$. At the UQCISD(T)(fc)/6-31G*/UMP2(full)/6-31G* level of theory Glukhovtsev and Schleyer¹ obtained a BDE = 29.5 kcal mol $^{-1}$ for the pyramid. Our values of 36.7 and 33.0 kcal mol $^{-1}$ obtained using the B3P86 and B3PW91 methods are in good agreement with these literature values. The calculations with the B3LYP method underestimate the BDE calculated with the higher level methods as only a BDE = 23.8 kcal mol $^{-1}$ was found. The calculated bond distances from ref 2 are $r_{12} = 3.054$ Å and $r_{15} = 3.121$ Å. The calculated bond distances for the pyramidal structure by Glukhovtsev and Schleyer are almost identical to the ones from ref 2 ($r_{12} = 3.065$ Å and $r_{15} = 3.145$ Å), values which are slightly longer than the ones we find.

In addition to the pyramidal structure, Glukhovtsev and Schleyer also investigated the bipyrmaidal sextet structure, but at a lower level of theory of UHF/3-21G//UHF/3-21G. This conformation lies 4.7 kcal mol $^{-1}$ higher in energy than the pyramid, a value which is substantially higher than our values of 0.8 kcal mol $^{-1}$ (B3LYP), 1.0 kcal mol $^{-1}$ (B3P86) and 1.0 kcal mol $^{-1}$ (B3PW91). The reason may be that our bipyrmaidal calculations converged toward a ${}^6A_2''$ state whereas the UHF calculations converged to a ${}^6A_1'$ state. Nevertheless, their frequency calculation gave two imaginary frequencies, a value which matches our obtained result. The electronic state in our calculations consists of five doubly occupied 1s orbitals and five singly occupied 2s orbitals. The latter five orbitals have a_1' , a_1' , a_2'' , e' , and e' symmetry giving an overall electronic state of ${}^6A_2''$. Thus, our obtained wave function is a "nonbonding" electronic state whereas the result calculation of Glukhovtsev and Schleyer possibly is an excited sextet state.

Two more conformations with zero imaginary frequencies have been found, namely the linear and cyclic structures, and therefore are local minima. All other structures have at least one imaginary frequency and therefore will be saddle points.

The most stable low spin configuration was found as the saw^{3,4} but in more recent calculations the bipyrmaid was found to be more stable.¹⁰ At the sextet spin state both these structures are transitions states with two imaginary frequencies in both cases.

3.5. ${}^7\text{Li}_6$. Full optimization of 13 isomeric heptet lithium hexamers have been performed using the B3LYP, B3P86 and B3PW91 methods. The investigated structures are a linear configuration ($D_{\infty h}$ symmetry), a cyclic configuration (D_{6h} symmetry), an octahedral (O_h symmetry), a diamond (D_{4h} symmetry), a prism (D_{3h} symmetry), a star (D_{3h} symmetry), 2,3-buta-lithium (D_{2h} symmetry), a propellor (D_{2d} symmetry), a pyramid (C_{5v} symmetry), a rectangular diamond (C_{2v} symmetry), a cheese (C_{2v} symmetry), a chair (C_{2h} symmetry), and a wobbly chair (C_i symmetry). Optimized geometries can be found in Figure 3 with bonding energies in Table 5.

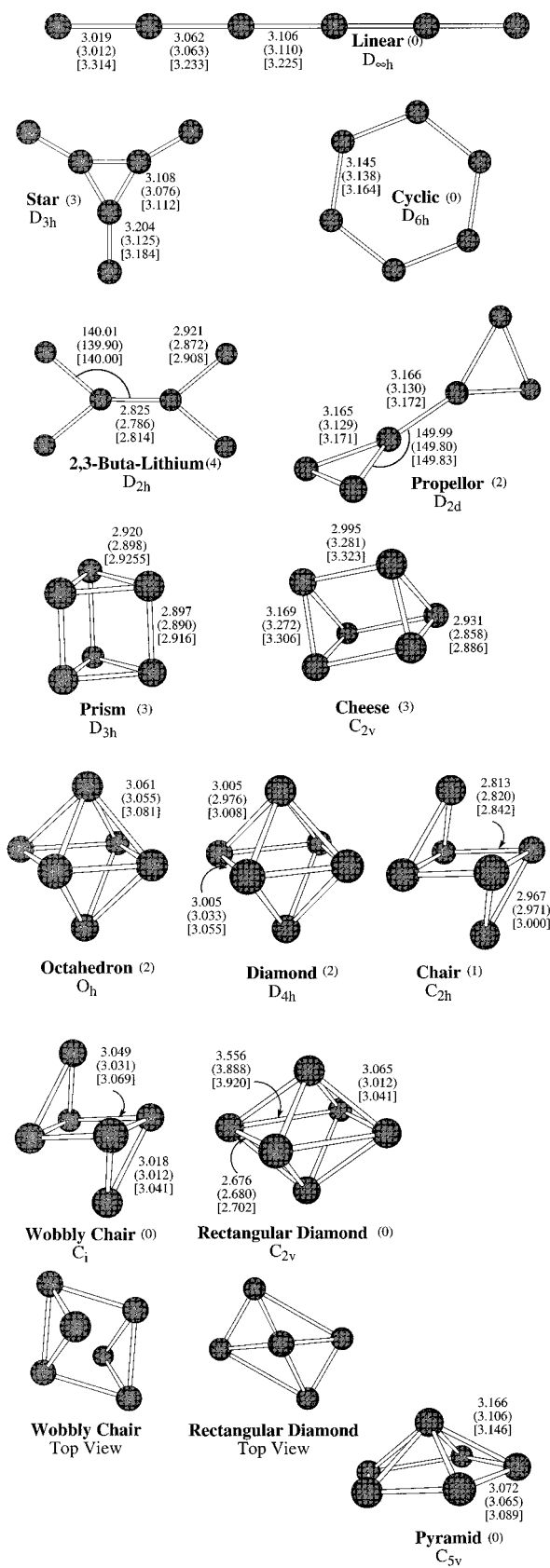


Figure 3. Optimized ${}^7\text{Li}_6$ structures with bond distances in angstroms calculated with B3LYP, B3P86 (brackets), and B3PW91 (square brackets).

The calculations of Glukhovtsev and Schleyer¹ showed that the diamond structure with D_{4h} symmetry was the lowest energy structure, although using their smallest basis set of 3-21G this structure gave two imaginary frequencies. At a higher level of

TABLE 5: Energies and Bond Dissociation Energies (BDE) of Different ${}^7\text{Li}_6$ Geometries^a

	B3LYP BDE (kcal mol ⁻¹)	B3P86 BDE (kcal mol ⁻¹)	B3PW91 BDE (kcal mol ⁻¹)
2,3-buta ${}^7\text{B}_{3u}$, D_{2h} (4) ^b	11.7	23.6	19.8
star ${}^7\text{A}_1'$, D_{3h} (3) ^c	14.9	24.5	21.2
linear ${}^7\Sigma_u$, $D_{\infty h}$ (0)	14.4	22.6	22.7
propellor ${}^7\text{A}_1$, D_{2d} (2) ^d	16.5	27.3	23.8
cheese ${}^7\text{A}_1$, C_{2v} (3) ^e	23.1	37.2	33.0
cyclo ${}^7\text{B}_{2u}$, D_{6h} (0) ^f	31.6	41.6	37.5
diamond ${}^7\text{B}_{1u}$, D_{4h} (2)	26.5	43.7	38.7
prism ${}^7\text{A}_2'$, D_{3h} (3)	27.8	43.8	38.9
octahedral ${}^7\text{T}_{1u}$, O_h (2)	26.2	43.9	39.1
pyramid ${}^7\text{A}_1$, C_{5v} (0)	31.5	46.4	41.8
chair ${}^7\text{B}_u$, C_{2h} (1)	30.0	47.6	42.8
wobbly chair ${}^7\text{A}_u$, C_i (0) ^g	33.0	50.5	45.6
rectangular ${}^7\text{A}_1$, C_{2v} (0)	33.0	50.5	45.6

^a For structures see Figure 3. Near each structure the number in parentheses correspond to the number of imaginary frequencies. ^b B3LYP gave two imaginary frequencies. ^c B3LYP gave two imaginary frequencies and B3P86 gave 5 imaginary frequencies. ^d B3P86 gave four imaginary frequencies. ^e B3LYP gave four imaginary frequencies. ^f B3LYP gave four imaginary frequencies. ^g B3LYP gave one imaginary frequency.

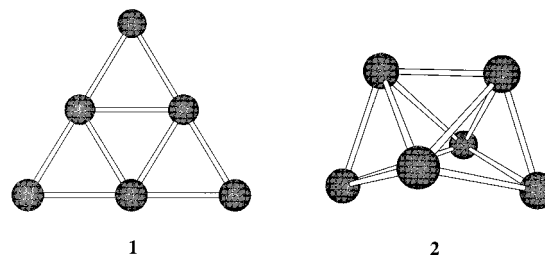
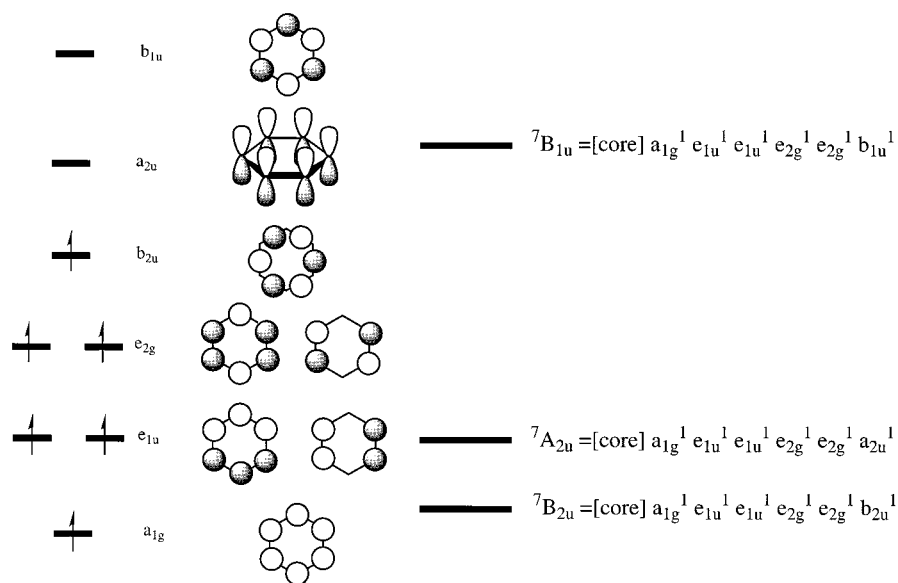


Figure 4. Tested Li_6 configurations **1** and **2**.

6-31G* no negative frequencies were obtained. Our calculations on this particular geometry gave two imaginary frequencies using all the different methods. Increasing the symmetry to O_h , however, still gave two imaginary frequencies. Lowering of the symmetry to a chair conformation with C_{2v} symmetry reduced the number of imaginary frequencies to one. The final structure without negative frequencies was found by taking the optimized chair configuration plus the Cartesian coordinates of the normal mode of the imaginary frequency. This structure is assigned as the wobbly chair. The point group symmetry reduced from C_{2v} to C_i symmetry on going from the chair to the wobbly chair configuration. A frequency calculation on the optimized wobbly chair geometry indeed gave positive frequencies only, indicating that it is a real minimum. At the B3LYP/cc-pVDZ level of theory, the chair and wobbly chair almost have octahedral symmetry, although the chair and wobbly chair are lower in energy to the octahedron by 3.8 and 6.8 kcal mol⁻¹, respectively. All other methods have significant differences between axial and equatorial bond distances, so that the geometries are clearly distorted from octahedral symmetry. The wobbly chair is 6.6 kcal mol⁻¹ and 6.5 kcal mol⁻¹ more stable than the octahedral symmetrical structure using the B3P86 and B3PW91 methods, respectively.

In the singlet spin the two lowest energy configurations have D_{3h} and C_{2v} symmetry.¹⁰ These structures have been schematically depicted in Figure 4 and are assigned **1** and **2**. Attempts to optimize these structures with septuplet spin failed. Structure **2** converged toward a rectangular diamond with C_{2v} symmetry and is very close in geometry to a D_{2h} symmetrical structure. Attempts to optimize this structure under D_{2h} symmetrical constraint failed due to a lowering of symmetry during the

SCHEME 2



optimization procedure. The rectangular diamond has substantially longer bonds than the diamond of up to 3.920 Å using the B3PW91 method. The B3LYP results, on the contrary, give much smaller bonds of 3.556 Å.

Surprisingly, the most stable septuplet lithium hexamer is a degenerate pair of isomeric structures formed by the wobbly chair and the rectangular diamond. All three investigated methods (B3LYP, B3P86, and B3PW91) give identical energies and bond dissociation energies for these two isomers (see Table 5). The frequency analyses shows that both states are real minima on the potential energy surface as no negative frequencies were found. Three more local minima with positive frequencies have been obtained, namely, the pyramid, the cyclic, and the linear conformations. The pyramidal structure lies 3.8 kcal mol⁻¹ higher in energy as the wobbly chair at the B3PW91/cc-pVDZ level of theory.

Glukhovtsev and Schleyer¹ investigated two isomers of septuplet lithium hexamer, namely the cyclic structure (D_{6h} symmetry) and the diamond (D_{4h} symmetry). The latter one was calculated at the UQCISD(T)(fc)/6-31G*/UMP2(full)/6-31G* level of theory and gave a bond dissociation energy of 34.1 kcal mol⁻¹. The cyclic isomer was found to have six imaginary frequencies at UHF/3-21G/UHF/3-21G level of theory and was 16.9 kcal mol⁻¹ higher in energy than the diamond. Our initial calculations on the cyclic compound in the $^7A_{2u}$ electronic state gave the same amount of imaginary frequencies for the cyclic structure but the energy gap between the cyclic and diamond structures is substantially lower. At B3LYP level the energy gap reduces to 6.2 kcal mol⁻¹, whereas the B3P86 and B3PW91 methods give a somewhat closer value of 12.3 kcal mol⁻¹ and 11.4 kcal mol⁻¹, respectively. In analogy to the quintet lithium tetramer, the heptet lithium hexamer has been recalculated in the $^7B_{2u}$ electronic state. This electronic state is comprised of six singly occupied σ orbitals. The highest singly occupied orbital has b_{2u} symmetry and has the electronic densities between the atomic centers and is built up by a linear combination of $2p_x$ and $2p_y$ orbitals and hence has a predominantly p-character. The $^7B_{2u}$ electronic state is substantially lower in energy than the $^7A_{2u}$ electronic state by 11.3 kcal mol⁻¹ (B3LYP), 10.2 kcal mol⁻¹ (B3P86), and 10.2 kcal mol⁻¹ (B3PW91). The order of the orbitals of the heptet lithium hexamer is schematically depicted on the left-hand-side of Scheme 2. The right-hand-

TABLE 6: Bond Dissociation Energies (BDE) in kcal mol⁻¹ of the Most Stable $^{n+1}Li_n$ Geometries^a

	method, basis set, from				
	B3LYP, cc-pVDZ, this work	B3P86, cc-pVDZ, this work	B3PW91, cc-pVDZ, this work	UQCISD(T), 6-31G*, ref 1	UCCSD(T), cc-pVDZ, ref 2
3Li_2 ($D_{\infty h}$)	0.4	1.7	1.3	0.6	0.7
4Li_3 (D_{3h})	6.2	11.0	9.4	7.9	10.2
5Li_4 (T_d)	20.1	29.8	27.1	25.3	29.6
6Li_5 (C_{4v})	23.8	36.7	33.0	29.5	35.4
7Li_6 (C_i) ^b	33.0	50.5	45.6	34.1	42.6

^a The symmetry of the calculated structure is written in brackets.

^b References 1 and 2 calculated a diamond structure with D_{4h} symmetry, explanation see text.

side of Scheme 2 gives the relative ordering of different low-lying electronic states. In conclusion, the electronic state calculated by Glukhovtsev and Schleyer¹ is an excited state while the lowest electronic state is the $^7B_{2u}$ state. The $^7B_{2u}$ cyclic conformer is a local minimum with positive frequencies only.

At the UCCSD(T)/cc-pVDZ level of theory, Danovich et al.² calculated the 7Li_6 in the O_h (octahedral) and D_{4h} (diamond) symmetrical orientations. The D_{4h} symmetrical structure produced a bond dissociation energy of 42.6 kcal mol⁻¹ and interatomic bond distances of $r_{12} = 3.122$ Å and $r_{15} = 3.125$ Å. These values were almost identical to the bond distance found for the octahedral hexamer of 3.125 Å. The interatomic distances we obtained for the octahedral symmetry are very close to the ones of Danovich et al., see Figure 3. Our calculations using the B3LYP method also give almost identical axial and equatorial bond distances for the diamond structure, but the discrepancies between the axial and equatorial bonds are somewhat larger using the B3P86 and B3PW91 methods.

4. Discussion

The most stable $^{n+1}Li_n$ ($n = 2-5$) clusters are the linear (3Li_2), the equatorial triangle (4Li_3), tetrahedral (5Li_4), and pyramidal (6Li_5) structures. The hexamer has a degenerate pair of minimum energy structures with C_i and C_{2v} symmetry. Bond dissociation energies of the most stable $^{n+1}Li_n$ clusters have been assembled in Table 6. In addition, the energies calculated at the UQCISD(T,fc)/6-31G*/UMP2(full)/6-31G* level of theory from ref 1

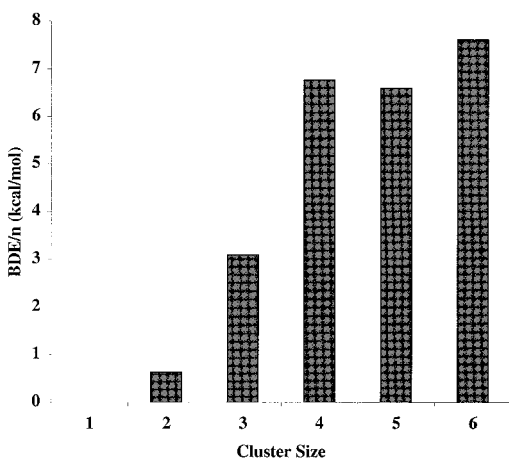


Figure 5. Relative bond dissociation energies (BDE/n) of Li_n , $n = 2-6$, clusters as a function of the cluster size using the calculations at the B3PW91/cc-pVDZ level of theory.

and the results from ref 2 at the UCCSD(T,full)/cc-pVDZ level of theory have been added to Table 6. As can be seen from Table 6, the bond dissociation energies calculated with the B3P86 and B3PW91 methods are in good agreement with the high level ab initio calculations from ref 1 and 2. Therefore, the B3P86 and B3PW91 methods are the most suitable density functional methods for the study of high-spin alkali metal clusters.

The relative bond dissociation energy (BDE/n) is defined as the total bond dissociation energy (BDE) divided by the total number of lithium atoms (n) in the cluster. Relative bond dissociation energies usually grow gradually until they reach a plateau of stability.⁷ In Figure 5 the relative bond dissociation energy has been plotted as a function of cluster size for the B3PW91 results for the most stable clusters ranging from Li_2 to Li_6 . The most stable clusters were linear (${}^3\text{Li}_2$), equilateral triangle (${}^4\text{Li}_3$), pyramidal (${}^5\text{Li}_4$), pyramidal (${}^6\text{Li}_5$), and wobbly chair (${}^7\text{Li}_6$), vide supra. The relative bond dissociation energies of lithium clusters (${}^{n+1}\text{Li}_n$, $n = 2-6$) as plotted in Figure 5 show an increase with the size of the cluster. This is in agreement with low-spin results from the literature (refs 3, 7, and 11). Obviously, the plateau of maximum stability has not been reached yet for a cluster size of six atoms.

In a previous paper of our group,² we used a valence bond (VB) method to elucidate the origins of “no-pair bonding” in ${}^3\text{Li}_2$ (${}^3\Sigma_u^+$). It was concluded that the bonding energy arises from the resonance interaction between the repulsive covalent triplet structure and the triplet charge-transfer structure. The number of available triplet charge-transfer structures increases with the cluster size and with the coordination number of each Li atom. As such, the VB model predicts a maximum dissociation energy for isomers with a maximum coordination number. Therefore, in Figure 6 the bond dissociation energies of the most stable lithium clusters have been plotted as a function of the total coordination number. For comparison the results from ref 1 and 2 have been added to the graph. The validity of the valence bond model is indicated by Figure 6, where an increase of the total number of bonds leads to an enhanced bond dissociation energy.

Further support for the model comes from Figure 7, in which the bond dissociation energies of all lithium hexamers studied here have been plotted as a function of the total number of lithium–lithium linkages. As can be seen from this figure, the BDE goes gradually up with rising amount of interatomic bonds. Consequently, the BDE of “no-pair bonded” lithium clusters is

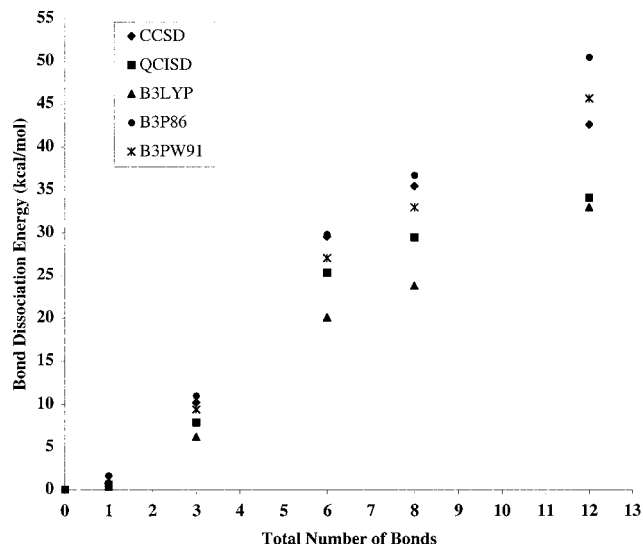


Figure 6. Bond dissociation energies for ${}^{n+1}\text{Li}_n$ as a function of the total coordination number of the most stable forms.

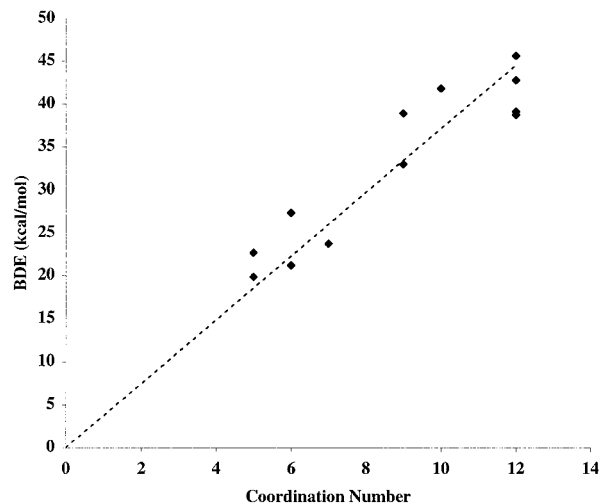


Figure 7. Bond dissociation energies of Li_6 clusters as a function of the total number of bonds within each isomer. All geometries were optimized at the B3PW91/cc-pVDZ level of theory.

indeed maximized for clusters with a maximum amount of lithium bonds. Moreover, it indicates that the model presented in ref 2 is an appropriate description of “no-pair bonding” in small lithium clusters in the high spin state.

5. Concluding Remarks

Density functional theory calculations have been performed on high spin lithium clusters. Many geometrical clusters have been considered. Two local ${}^4\text{Li}_3$ minima have been found with $D_{\infty h}$ and D_{3h} symmetry, respectively. The latter one has been found to be the most stable form. In the quintet state four stable tetramers have been found. With increasing stability these isomers have symmetry: $D_{\infty h}$, C_{2v} , D_{4h} , and T_d . Also three stable sextet lithium pentamers have been calculated, namely the linear, cyclic and pyramidal forms. As many as five different local minima on the ${}^7\text{Li}_6$ potential energy surface have been located. The stable forms have symmetry groups: $D_{\infty h}$, D_{6h} , C_{5v} , C_i , and C_{2v} . The latter two form a degenerate pair of minimum energy structures. In particular, it should be pointed out that all linear and cyclic ${}^{n+1}\text{Li}_n$ structures studied here were found to be local minima.

A thorough study using different density functional methods, i.e. BLYP, BP86, BPW91, B3LYP, B3P86, and B3PW91, has

been performed. For the higher clusters, the BLYP, BP86, and BPW91 calculations give less reliable results as the Becke three-parameter calculations, especially with respect to UCCSD(T) calculations. Furthermore, these calculations often converge to the wrong electronic state and cannot reproduce the correct ground-state geometry. Therefore, the BLYP, BP86, and BPW91 methods are shown to be less suitable for the study of high-spin lithium clusters. The B3LYP calculations underestimate the bond dissociation energy quite considerably, whereas the B3P86 and B3PW91 methods can reproduce bond dissociation energies calculated with UCCSD(T)/cc-pVDZ excellently. In conclusion, the most suitable density functional methods for the study of high spin lithium clusters are the B3P86 and B3PW91 methods. Calculations using different basis sets have been shown that the smallest basis set, i.e., cc-pVDZ, is quite suitable. Of deemed importance is the addition of p-functions as the high spin clusters very often have a highest singly occupied σ -orbital which is a linear combination of $2p_x$ and $2p_y$ atomic orbitals and therefore has a dominant p-character.^{1,2}

Trends show that the total bond dissociation energy of “no-pair” clusters follows the predictions of the VB model and is dependent on the maximum number of bonds within the cluster and therefore the system with the highest symmetry number usually is the lowest energy structure. The bond which originates in the mixing of all the available charge-transfer configurations² into the repulsive high-spin covalent structure, is best viewed as a collective bond delocalized over the entire cluster via adjacent ionic fluctuations. The origin of the binding, therefore, comes from the triplet (multiplet) interactions within the system. Density Functional Methods studied here are in good agreement with UQCISD(T) and UCCSD(T) calculations,^{1,2} and can therefore serve in future studies of larger clusters with an attempt to establish asymptotic properties at $n \rightarrow \infty$.

Acknowledgment. This research was supported by the Robert Szold Fund.

Supporting Information Available: Seven tables with total energies of all optimized geometries. This material is available free of charge via the Internet at <http://pubs.acs.org>.

References and Notes

- (1) Glukhovtsev, M. N.; von Ragué Schleyer, P. *Isr. J. Chem.* **1993**, *33*, 455.
- (2) Danovich, D.; Wu, W.; Shaik, S. *J. Phys. Chem. A* **1999**, *121*, 3165.
- (3) Boustani, L.; Pewestorf, W.; Fantucci, P.; Bonacic-Koutecky, V.; Koutecky, J. *Phys. Rev. B* **1987**, *35*, 9437.
- (4) Rao, B. K.; Khanna, S. N.; Jena, P. *Phys. Rev. B* **1987**, *36*, 953.
- (5) Förner, W.; Seel, M. *J. Chem. Phys.* **1987**, *87*, 443.
- (6) (a) McAdon, M. H.; Goddard, W. A., III *J. Phys. Chem.* **1987**, *91*, 2607. (b) McAdon, M. H.; Goddard, W. A., III *J. Phys. Chem.* **1988**, *92*, 1352. (c) McAdon, M. H.; Goddard, W. A., III *J. Chem. Phys.* **1987**, *88*, 277.
- (7) Bonacic-Koutecky, V.; Fantucci, P.; Koutecky, J. *Chem. Rev.* **1991**, *91*, 1035.
- (8) Blanc, J.; Bonacic-Koutecky, V.; Broyer, M.; Chevalyere, J.; Dugourd, Ph.; Koutecky, J.; Scheuch, C.; Wolf, J. P.; Wöste, L. *J. Chem. Phys.* **1992**, *96*, 1793.
- (9) Jellinek, J.; Bonacic-Koutecky, V.; Fantucci, P.; Wiechert, M. *J. Chem. Phys.* **1994**, *101*, 10092.
- (10) Gardet, G.; Rogemond, F.; Chermette, H. *J. Chem. Phys.* **1996**, *105*, 9933.
- (11) Jones, R. O.; Lichtenstein, A. I.; Hutter, J. *J. Chem. Phys.* **1997**, *106*, 4566.
- (12) *Gaussian 98*, Revision A.7; Gaussian Inc.: Pittsburgh, PA, 1998.
- (13) Becke, A. D. *Phys. Rev. A* **1988**, *38*, 3098.
- (14) Becke, A. D. *J. Chem. Phys.* **1993**, *98*, 5648.
- (15) Perdew, J. P. *Phys. Rev. B* **1986**, *33*, 8822.
- (16) Lee, C.; Yang, W.; Parr, R. G. *Phys. Rev. B* **1988**, *37*, 785.
- (17) Perdew, J. P.; Wang, Y. *Phys. Rev. B* **1992**, *45*, 13244.
- (18) Dunning, T. H., Jr. *J. Chem. Phys.* **1989**, *90*, 1007.
- (19) Woon, D. E. Private communication.